Indian Journal of Science and Technology, *Vol 9(37), DOI: 10.17485/ijst/2016/v9i37/88464, October 2016*
ISSN (Print) : 0974-6846
ISSN (Online) : 0974-5645

A 4-ary Control Algorithm for Direct Power Control of Three Phase Pulse Width Modulated Rectifier

Mahedihusain A. Lokhandwala[1]* and Hina B. Chandwani[2]

[1]V. T. Patel Department of Electronics and Communication Engineering, Faculty of Technology and Engineering, Charotar University of Science and Technology, Changa - 388421, Gujarat, India; mal_piet@yahoo.co.in
[2]Department of Electrical Engineering, Faculty of Technology and Engineering, Maharaja Sayajirao University of Baroda, Vadodara - 390020, Gujarat, India

Abstract

Objectives: The Direct Power Control (DPC) strategy for front end Pulse Width Modulated (PWM) rectifier employing binary hysteresis controller with two digital outputs and a new 4-ary control algorithm with four digital outputs is investigated. **Methods/Analysis:** The prototype DPC-PWM rectifier based on conventional binary algorithm and proposed 4-ary control algorithm for hysteresis controllers is designed and modeling and simulation was performed in MATLAB/SIMILINK® environment. The total harmonic distortion of supply current and average switching frequency under steady state are measured for a load of wide dynamic range for different hysteresis widths. The DC output voltage ripples and power ripples are also observed. **Findings:** It was found that the total harmonic distortion in supply current was reduced and remained bounded within narrow range in 4-ary control as compared to binary control. The average switching frequency also remained bounded within narrow range in proposed control as compared to conventional hysteresis control. The DC output voltage ripples and power ripples were found to be reduced considerably at heavy loads as compared to binary control. **Novelty/Improvement:** The tight control of active and reactive powers not only around the hysteresis band but also within the hysteresis band is achieved with simple algorithm.

Keywords: Direct Power Control, DPC, 4-ary Algorithm, Front End Rectifier, Improved DPC, Pulse Width Modulated Rectifier

1. Introduction

Various methods have been proposed for control of powers in PWM rectifiers[1–20] which can be broadly classified as indirect power control or Direct Power Control methods. The major problem of simple, fast and accurate Hysteresis Current Control (HCC) is that its average and instantaneous switching frequencies vary with the DC load current causing excessive stress on switching devices[2]. The Voltage-Oriented Control (VOC)[3–9] for indirect power control offers high dynamics and static performance via internal current control loops. However, the final configuration and performance of the VOC system largely depends on the quality of the applied current control strategy[4–6]. Another method developed analogous to direct torque control used for adjustable speed drives is direct power control[10–20].

The control technique using instantaneous active and reactive power rather than current was first proposed by[10]. Subsequently[11] named it as Direct Power Control. In this hysteresis controller based DPC, a proper switching vector is selected from Switching Table (ST), and applied during the next control period on the basis of outputs of hysteresis controllers and position of the supply line voltage space vector which is termed as ST-DPC.

Much research has been carried out to improve the performance of the DPC. The Virtual Flux based DPC (VF-DPC)[12] and DPC using Space Vector Modulation (DPC-SVM)[13] were aimed at improving the performance under unbalance and pre-distorted grid at constant switching frequency. May researchers have proposed different switching tables[15–18] to reduce the Total Harmonic Distortion (THD) of line currents and the switching

*Author for correspondence

losses. The duty cycle based control was also proposed which reduces power ripples and supply current THD[19]. But the performance over the wide range of load current is required to be addressed. In many applications, like industrial motor drives, air conditioning etc, the load current varies significantly over a wide range. Hence, the rectifier designed to power such applications must be able to provide satisfactory control over wide dynamic range of load current. The THD of the supply line current is inversely proportional to the line inductance and switching frequency for PWM rectifier. The maximum permissible value of inductance is inversely proportional to the load current[4]. If high value of inductance is employed then the DC output voltage will have high amount of ripple or even may not built up to the desired value. If significantly low inductance is employed then the current ripples at low load current increases and consequently THD increases. It is not possible to vary the inductance for optimum performance over wide load current range. Hence, there is a need for a control strategy which may allow satisfactory operation of rectifier over a wide dynamic range of load current.

This paper proposes a control algorithm which provides control within the hysteresis band also, for tight control of instantaneous active and reactive power, to improve the performance over wide dynamic range of load current. An overview of the conventional Direct Power Control strategy is presented in Section 2. In Section 3, the instantaneous power within hysteresis band is analyzed and a new control technique is developed for power control within hysteresis band. The simulation and result analysis for DPC-PWM rectifier based on conventional and proposed 4-ary control algorithm for hysteresis control is discussed in Section 4.

2. Conventional Direct Power Control Strategy

Figure 1 shows schematic diagram of Direct Power Control of 3-ph PWM active rectifier. Following notations are used:

e_a, e_b, e_c instantaneous three-phase supply voltages,

i_a, i_b, i_c instantaneous three-phase line currents,

v_a, v_b, v_c instantaneous ac side converter voltages,

i_o, i_L instantaneous converter output current and load current,

L, R boost inductance and its resistance,

C, R_L filter capacitor and equivalent load resistance,

$v_o = V_{dc}$ converter dc side voltage,

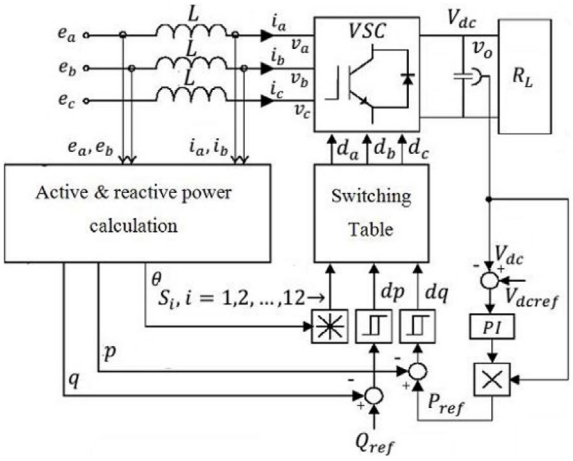

Figure 1. Schematic diagram of ST-DPC scheme.

In DPC strategy, the instantaneous active power p and reactive power q are computed at every sampling instant and compared with the desired reference values P_{ref} and Q_{ref} using hysteresis comparators. If the error is above or below the tolerable limits, appropriate digital control signals are generated as shown below:

$$\left.\begin{array}{ll} dp = 1 & \Delta p = P_{ref} - p > {}^{H_{WP}}/_{2} \\ = 0 & \Delta p = P_{ref} - p < -{}^{H_{WP}}/_{2} \\ = \text{no change} & -{}^{H_{WP}}/_{2} \le \Delta p \le {}^{H_{WP}}/_{2} \end{array}\right\} \quad (1)$$

and

$$\left.\begin{array}{ll} dq = 1 & \Delta q = Q_{ref} - q > {}^{H_{WQ}}/_{2} \\ = 0 & \Delta q = Q_{ref} - q < -{}^{H_{WQ}}/_{2} \\ = \text{no change} & -{}^{H_{WQ}}/_{2} \le \Delta q \le {}^{H_{WQ}}/_{2} \end{array}\right\} \quad (2)$$

The stationary coordinates are divided into 12 sectors as shown in Figure 2. The switching table is prepared containing switching vectors as a function of two digital

Table 1. Improved switching table by Baktash et. al[17]

dp	dq	S_1	S_2	S_3	S_4	S_5	S_6	S_7	S_8	S_9	S_{10}	S_{11}	S_{12}
1	1	V_7	V_7	V_0	V_0	V_7	V_7	V_0	V_0	V_7	V_7	V_0	V_0
1	0	V_6	V_7	V_1	V_0	V_2	V_7	V_3	V_0	V_4	V_7	V_5	V_0
0	1	V_1	V_2	V_2	V_3	V_3	V_4	V_4	V_5	V_5	V_6	V_6	V_1
0	0	V_6	V_1	V_1	V_2	V_2	V_3	V_3	V_4	V_4	V_5	V_5	V_6

outputs of the hysteresis comparators and twelve sectors. Optimum switching vector is selected depending upon two digital outputs and location of supply voltage vector to reduce errors Δp and Δq . The switching table proposed by[11] is termed as classical switching table. The new switching tables are proposed to improve the performance of the DPC method[15–18]. The switching table proposed by[17] offers good performance which is shown in Table 1.The primary focus of these works was to reduce the Total Harmonic Distortion (THD) of line currents and the switching losses. The performance over the wide load current range was not considered.

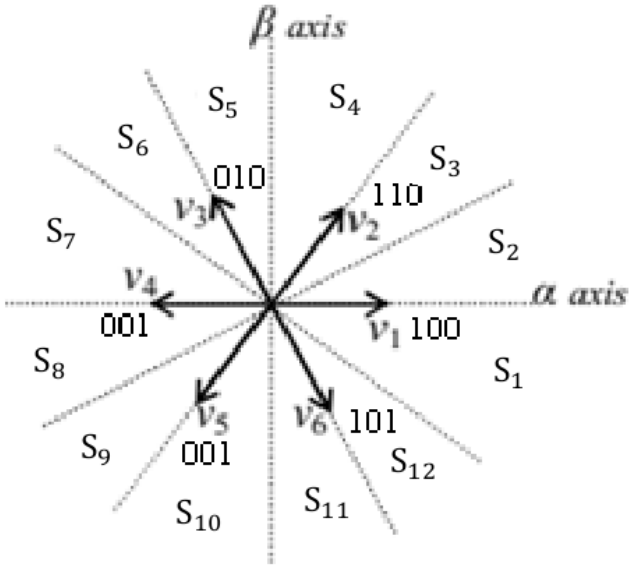

Figure 2. Switching vectors of converter and sectors of stationary coordinates.

3. Power Control within Hysteresis Band (4-ary Algorithm)

The conventional hysteresis controllers described by Equation (1) and (2) do not provide control of powers within hysteresis band. The next switching vector is applied only after the instantaneous power crosses hysteresis band. The time taken by power to cross hysteresis band is a complicated function of output DC voltage (V_{dc}), energy stored in inductor (W_L), instantaneous value of supply voltage (e), time constant of the inductor ($\tau = {}^{L}/_{R}$) and the width of hysteresis band (H_W), if source and switch resistances are neglected. If the time taken by power to cross the hysteresis band is denoted by T_h and control period by T_c, then the hysteresis band will be swept in less than one control period if Equation (3) is satisfied.

$$T_c \geq T_h \tag{3}$$

But the switching control period T_c employed is practically much smaller than T_h because sufficiently high switching frequencies are employed to control the harmonics within limit. Hence, it may take more than one control periods for instantaneous power to cross the hysteresis band only after which the next switching vector can be applied in conventional hysteresis controller.

The performance during hysteresis band can be improved if T_h can be adjusted such that it approaches the value of T_c. But changing T_h requires change in one or more of the parameters V_{dc}, W_L, e, τ and H_W. The only parameter over which we have control is H_W. Figure 3 depicts the situation of powers outside and within hysteresis band $H_{WP} = \Delta p$, for active power controller. For T_h to approach T_c, H_{WP} is adjusted using 4-ary algorithm as shown in Figure 4. It is termed here as 4-ary algorithm, because hysteresis controller generates four levels at its output (four digital outputs). The algorithm shown in grey box is to control power within hysteresis band.

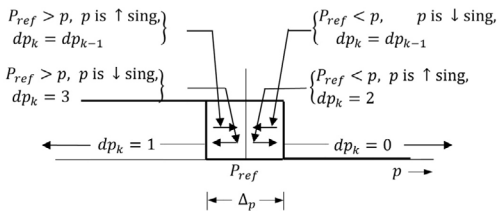

Figure 3. Active power within hysteresis band.

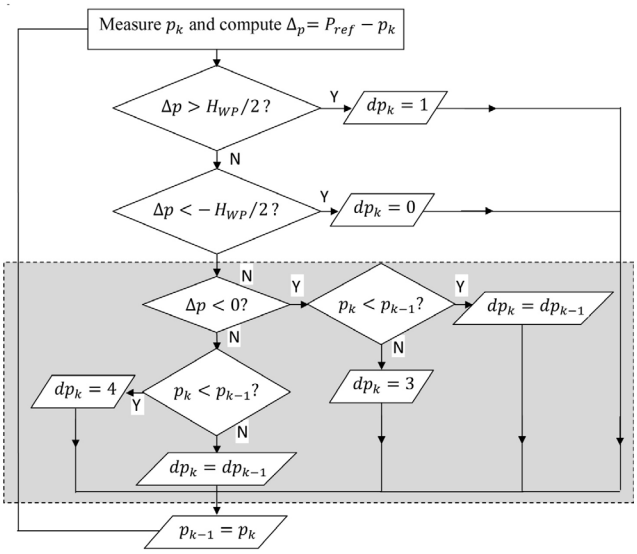

Figure 4. The 4-ary control algorithm.

When controller output dp_k is either **0** or **2**, the switching vector which decreases power is employed and when it is 1 or 3, the switching vector which increases power is employed. Similar comment is employed for controller output dq_k. Hence, 16-state switching table is required as shown in Table 2. In Table 2, the outputs $dp = \mathbf{2}$ and $dp = \mathbf{3}$ contain same rows for outputs $dp = \mathbf{0}$ and $dp = \mathbf{1}$ respectively. Similarly, rows for $dq = \mathbf{2}$ and $dq = \mathbf{3}$ contains the same switching vectors as in rows for $dq = \mathbf{0}$ and $dq = \mathbf{1}$. Hence, the 16-state switching vectors can be applied using two state switching table shown in Table 1 by using additional logic for ORing controller outputs. The schematics of the controller with additional logic for converting 4-ary output of hysteresis controllers to binary outputs is shown in figure 5 for active power control. The same type of algorithm and control logic as shown in Figure 4 and Figure 5 are employed for reactive power control also.

4. Simulation and Result Analysis

The conventional binary DPC and DPC with 4-ary control are simulated in MATLAB/SIMULINK environment. The switching table shown in Table 1 is employed in this

Table 2. Switching Table employing 4-Level control of active and reactive power

dp	*dq*	S_1	S_2	S_3	S_4	S_5	S_6	S_7	S_8	S_9	S_{10}	S_{11}	S_{12}
1	1	7	7	0	0	7	7	0	0	7	7	0	0
	0	5	6	6	1	1	2	2	3	3	4	4	5
	3	7	7	0	0	7	7	0	0	7	7	0	0
	2	5	6	6	1	1	2	2	3	3	4	4	5
0	1	1	2	2	3	3	4	4	5	5	6	6	1
	0	6	1	1	2	2	3	3	4	4	5	5	6
	3	1	2	2	3	3	4	4	5	5	6	6	1
	2	6	1	1	2	2	3	3	4	4	5	5	6
3	1	7	7	0	0	7	7	0	0	7	7	0	0
	0	5	6	6	1	1	2	2	3	3	4	4	5
	3	7	7	0	0	7	7	0	0	7	7	0	0
	2	5	6	6	1	1	2	2	3	3	4	4	5
2	1	1	2	2	3	3	4	4	5	5	6	6	1
	0	6	1	1	2	2	3	3	4	4	5	5	6
	3	1	2	2	3	3	4	4	5	5	6	6	1
	2	6	1	1	2	2	3	3	4	4	5	5	6

work as it gives the best results. The performance of conventional DPC using binary control algorithm and DPC with 4-ary algorithm is evaluated. The system specifications and control parameters are shown in Table 3.

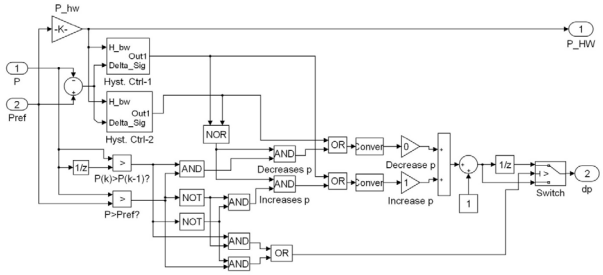

Figure 5. Simulink subsystem for controller output d_p shown in Figure 4.

Table 3. System specifications and control parameters

Specifications	Notation	Value
Supply phase voltage	e_a, e_b, e_c	$90/\sqrt{2}$ Vrms
Frequency	f	50 Hz
Connection		3-Ph, Y
Desired output voltage	V_{dc}	300 V
Control (Sampling) Interval	T_c	Adjusted (20 μs /25 μs)
Line Inductance	L	2 mH
Line Resistance	R	0.01 Ω
DC bus capacitor	C	4700 μF
Equi. Load Resistance	R_L	10 Ω, 5 Ω, 20 Ω, 3Ω applied in steps.

The simulation was run for different hysteresis widths of active and reactive powers and for two sampling frequencies ($F_s = {}^{1}/_{T_c}$) of 50 kHz and 40 kHz. The load resistance was varied during simulation as follows to test the performance over a wide dynamic range of load current.

$0 \le t < 0.5\ s \quad R_L = 10\ \Omega \quad I_{dc} = 30\ A$

$0.5 \le t < 1.2\ s \quad R_L = 5\ \Omega \quad I_{dc} = 60\ A$

$1.2 \le t < 1.8\ s \quad R_L = 20\ \Omega \quad I_{dc} = 15\ A$

$1.8 \le t < 2.5\ s \quad R_L = 3\ \Omega \quad I_{dc} = 100\ A$

The Total Harmonic Distortion (**THD**) and average switching frequency are considered as performance parameters. The THD was measured using 'Powergui' tool of MATLAB/SIMULINK. The gate pulse amplitudes at simulation times are stored in a structure and a script was run to note the gate pulse transitions and corresponding instants, using which average frequency was measured under steady state over 5 cycles of supply voltages for different loads. Figure 6 shows THD vs. hysteresis width as a percentage of P_{ref} with load current as a parameter for a given load and switching frequency. The THD varies considerably as a function of H_w for conventional hysteresis controller where as it remains bounded around the minimum possible value for 4-ary controller. This is because this algorithm tries to maintain the power within a minimum band which is a function of T_h and T_c once power enters into the band as discussed in Section 3. Increasing T_c from 2 μs to 2.5 μs , increases THD but it is maintained constant for change in H_w .

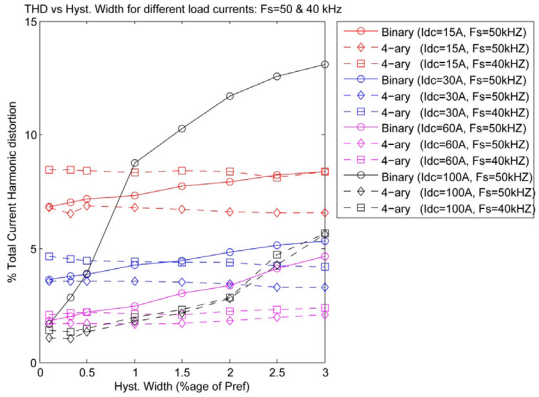

Figure 6. THD vs. hysteresis width for Different Load Currents.

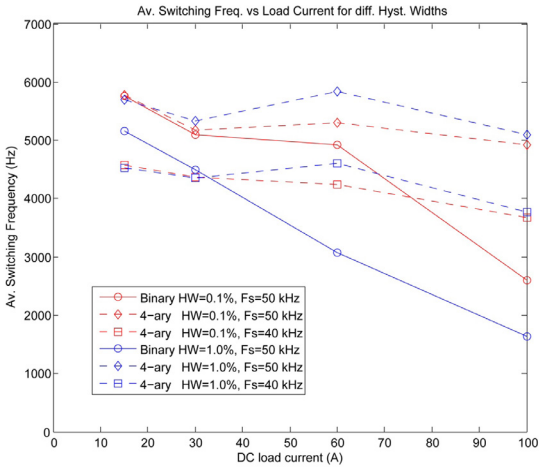

Figure 7. Average switching frequency vs. load current.

Figure 7 shows the average switching frequency vs. load current with sampling frequency (control period) as

a parameter. The average switching frequency was found to be inversely proportional to the load current in case of binary controller based DPC, whereas it was maintained within narrow range about a fixed value. As can be seen, the switching frequency can be controlled by varying control period (sampling frequency).

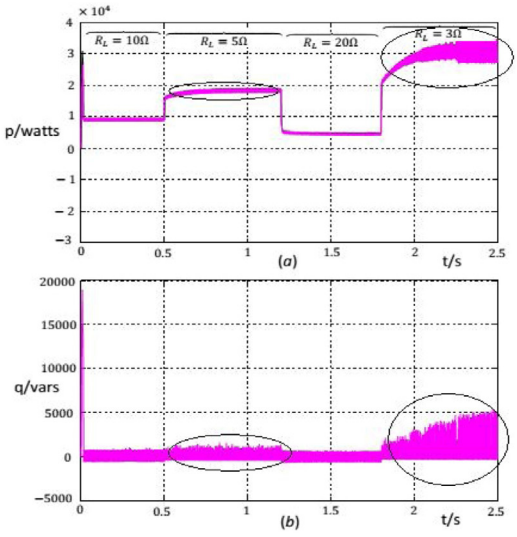

Figure 8. Instantaneous active (a) and reactive (b) power for conventional DPC.

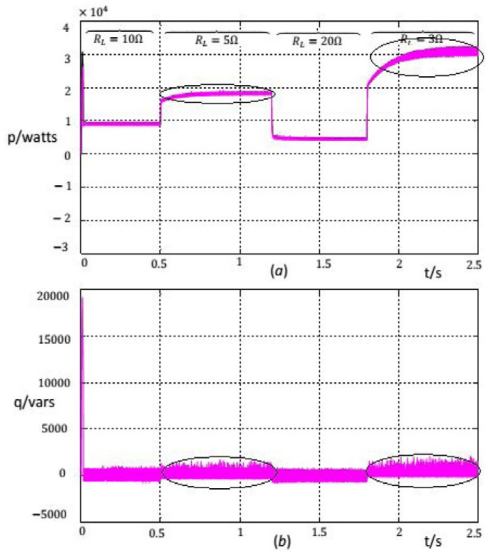

Figure 9. Instantaneous active (a) and reactive (b) power for DPC using proposed controller.

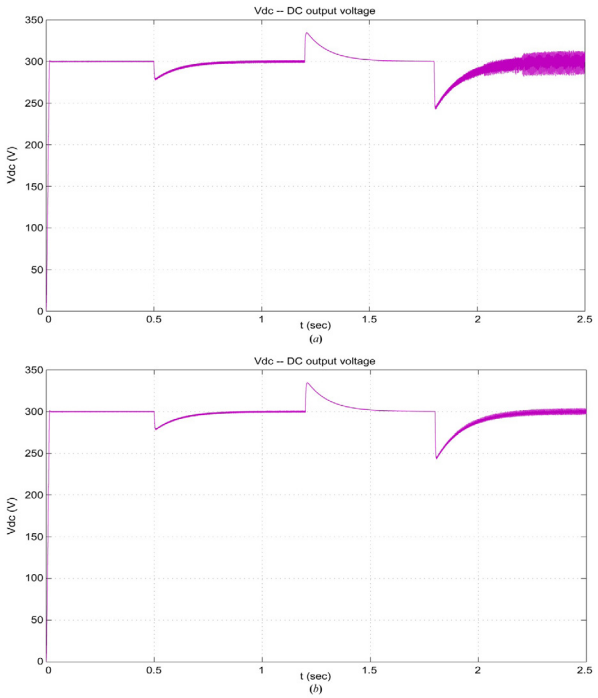

Figure 10. Output voltage for H_W =1% (a) Conventional DPC, (b) DPC employing 4-ary algorithm.

In Figures 8 and 9, instantaneous active and reactive powers are plotted for different loads for H_W = 1%. It is evident that the power ripples are quiet high for high load currents in case of conventional DPC whereas they are sufficiently reduced for DPC with 4-ary control. Figure 10 shows DC output voltage waveforms in which the voltage ripples are quiet reduced at higher load current of 60 A (0.5 to 1.2 sec) and 100 A (1.8 to 2.5 sec) for DPC with proposed algorithm.

5. Conclusions

In this paper, the new 4-ary algorithm for hysteresis controller is presented for tight control of power within hysteresis band.

The conventional DPC-PWM rectifiers using binary and DPC-PWM with 4-ary control were designed, modeled and simulated using MATLAB/SIMULINK. The THD of supply current increased/decreased as hysteresis width of powers increased/decreased for a given load current in case of conventional DPC, where as it remained almost constant for change in hysteresis width in case of DPC with 4-ary control. The switching frequency varied inversely as load current in conventional DPC whereas

it remained within a narrow range in DPC using 4-ary control. The power and DC voltage ripples were quiet high for high load currents in case of conventional DPC whereas they were sufficiently reduced for DPC with 4-ary control. This was because of the fact that the 4-ary algorithm tries to confine the active and reactive power within the hysteresis band and forces them to approach their reference value and also adjusts the hysteresis width to be minimum required for optimum performance.

Hence, PWM rectifier designed using DPC with 4-ary control can give better performance as compared to conventional binary DPC for applications where load current varies dynamically over wide ranges.

The implementation of proposed 4-ary algorithm is very simple hence the system complexity is not much increased. More accurate control can be achieved if the time taken by power to cross the hysteresis band can be calculated and further control is added.

6. References

1. Liserre M, Aquila AD, Blaabjerg F. An overview of three-phase voltage source active rectifiers interfacing the utility. IEEE Power Tech Conference Proceedings; Bologna, Italy. 2003 Jun 23-26.
2. Wu R, Dewan SB, Slemon GR. A PWM AC to DC converter with fixed switching frequency. IEEE Conference Proceedings of Industry Application Society Meeting. 1988 Oct; 1:706–11.
3. Jahns TM, Blasko V. Recent advances in power electronics technology for industrial and traction machine drives. Proceedings of the IEEE. 2001; 89(6):963–75.
4. Malinowski M. Sensorless control strategies for three-phase PWM rectifiers. [PhD Thesis]. Institute of Control and Industrial Electronics, Faculty of Electrical Engineering: Warsaw University of Technology; 2001.
5. Hansen S, Malinowski M, Blaabjerg F, Kazmierkowski MP. Control strategies for PWM rectifiers without line voltage sensors. Proceedings of IEEE APEC. 2000; 2:832–9.
6. Kazmierkowski MP, Malesani L. Current control techniques for three-phase voltage-source PWM converters: A survey. IEEE Transactions on Industrial Electronics. 1998 Oct; 45(5):691–703.
7. Kwon BH, Youm JH, Lim JW. A line-voltage-sensorless synchronous rectifier. IEEE Transactions on Power Electronics. 1999 Sept; 14(5):966–72.
8. Prasad JS, Bhavsar T, Ghosh R, Narayanan G. Vector control of three-phase AC/DC front-end converter. Sadhana. 2008 Oct; 33(5):591–613.
9. Bose Bimal K. Modern power electronics and AC Drives. 2nd ed. New Delhi: PHI Learning Private Limited; 2002.
10. Ohnishi T. Three phase PWM converter/inverter by means of instantaneous active and reactive power control. Proceedings of IEEE International Conference on Industrial Electronics, Control and Instrumentation IECON'91; 1991. p. 819–24.
11. Noguchi T, Tomiki H, Kondo S, Takahashi I. Direct Power Control of PWM converter without power-source voltage sensors. IEEE Transactions on Industry Applications. 1998 May-Jun; 34(3):473–9.
12. Malinowski M, Kazmierkowski MP, Hansen S, Blaabjerg F, Marques GD. Virtual-flux-based Direct Power Control of three-phase PWM rectifiers. IEEE Transactions on Industry Applications. 2001; 37(4):1019–27.
13. Malinowski M, Jasinski M, Kazmierkowski MP. Simple Direct Power Control of three-phase PWM rectifier using Space-Vector Modulation (DPC-SVM). IEEE Transactions on Industrial Electronics. 2004 Apr; 51(2):447–54.
14. Larrinaga S. Predictive control of the 2L-VSI and 3L-NPC VSI based on Direct Power Control for MV grid-connected power applications. [Ph. Thesis]. Mondragon, Espanha: Goi Eskola Politeknikoa Faculty of Engineering; 2007.
15. Wang J. Model predictive control of power electronics converter. [Master of Science Thesis]. Department of Electric Power Engineering, Norwegian University of Science and Technology; 2012.
16. Bouafia A, Gaubert JP, Krim F. Analysis and design of new switching table for Direct Power Control of three-phase PWM rectifier. Proceedings of IEEE 13th Power Electronics and Motion Control Conference, EPE-PEMC; 2008.
17. Baktash A, Vahedi A, Masoum M. Improved switching table for Direct Power Control of three-phase PWM rectifier. Proceedings of Australasian Universities Power Engineering Conference, AUPEC; 2007. p. 1–5.
18. Eloy-Garcia J, Alves R. DSP-based Direct Power Control of a VSC with voltage angle estimation. IEEE/PES Transmission and Distribution Conference and Exposition, TDC'06; Latin America. 2006. p.1–5.
19. Zhang Y, Li Z, Zhang Y, Xie W, Piao Z, Hu C. Performance improvement of Direct Power Control of PWM rectifier with simple calculation. IEEE Transactions on Power Electronics. 2013; 28(7):3428–37.
20. Hu J, Zhu J, Dorrell DG. In-depth study of Direct Power Control strategies for power converters. IET Power Electronics. 2014; 7(7):1810–20.